Journal of Fluorescence, Vol. 5, No. 4, 1995

Synthesis and Spectroscopic Studies of 4-Formyl-4'-*N*,*N*-dimethylamino-1,1'-biphenyl: The Unusual Red Edge Effect and Efficient Laser Generation

Pi-Tai Chou,[1,2,4] Chen-Pin Chang,[3] John H. Clements,[1] and Kuo Meng-Shin[3]

Received October 3, 1994; revised March 15, 1995; accepted March 27, 1995

The synthesis and photophysics of 4-formyl-4'-*N*,*N*-dimethylamino-1,1'-biphenyl are reported. The emission spectrum in various solvent polarities demonstrates solvatochromism, indicating that the fluorescence originates from an electronically excited species with a strong charge transfer character. The change in $\Delta\tilde{\nu}$ [$\tilde{\nu}_{max}$(absorption) − $\tilde{\nu}_{max}$(emission)] varies from ~1500 cm^{-1} in *n*-heptane to as much as ~7500 cm^{-1} in acetonitrile. In protic solvents, the unusual excitation energy-dependent steady-state emission (red edge effect), resulting from solvent dielectric relaxation, was observed in media with a low viscosity. The large Stokes-shifted and high-yield fluorescence led to the observation of the efficient lasing action. The frequency tunability of the laser output is strongly solvent dependent, generating a new charge transfer laser dye in the blue–green region.

KEY WORDS: Excited-state intramolecular charge transfer; red edge effect; amplified spontaneous emission; lasing action.

INTRODUCTION

The photophysics of organic molecules exhibiting excited-state intramolecular charge transfer (ESICT) properties have received considerable attention since the original observation of ESICT in *p*-dimethylaminobenzonitrile [1,2]. Recently, the use of ESICT molecules to probe solvation dynamics has also been studied extensively due to the rapid development of ultrafast time-resolved techniques in combination with molecular dynamics calculations assisted by fast computation capabilities [3–6]. From an application viewpoint, the use of the ESICT concept for constructing molecular assemblies capable of yielding unusual optical and electrical bulk properties has been proposed [7,8]. Supramolecules based on donor/acceptor aromatic systems in a small overlap arrangement, such as in the structure generalized as a polyphenyl system (e.g., **1** in Fig. 1), were proposed to be capable of switching between two macroscopically

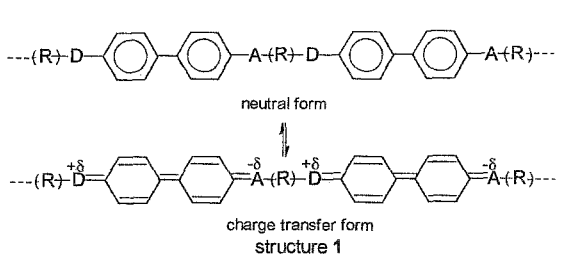

Fig. 1. Structures of the proposed supramolecule based on the D (donor)/A (acceptor)-substituted polybiphenyl system **1**. *R* can be a conducting $(-CH=CH-)_n$ group or an insulating spacer such as $(-CH_2-)_n$.

[1] Department of Chemistry and Biochemistry, University of South Carolina, Columbia, South Carolina 29208.
[2] Current address: Department of Chemistry, National Chung-Cheng University, Chia-Yi, Taiwan, R.O.C.
[3] Department of Chemistry, Fu-Jen Catholic University, Shin Chuang, Taiwan, R.O.C.
[4] To whom correspondence should be addressed.

1053-0509/95/1200-0369$07.50/0

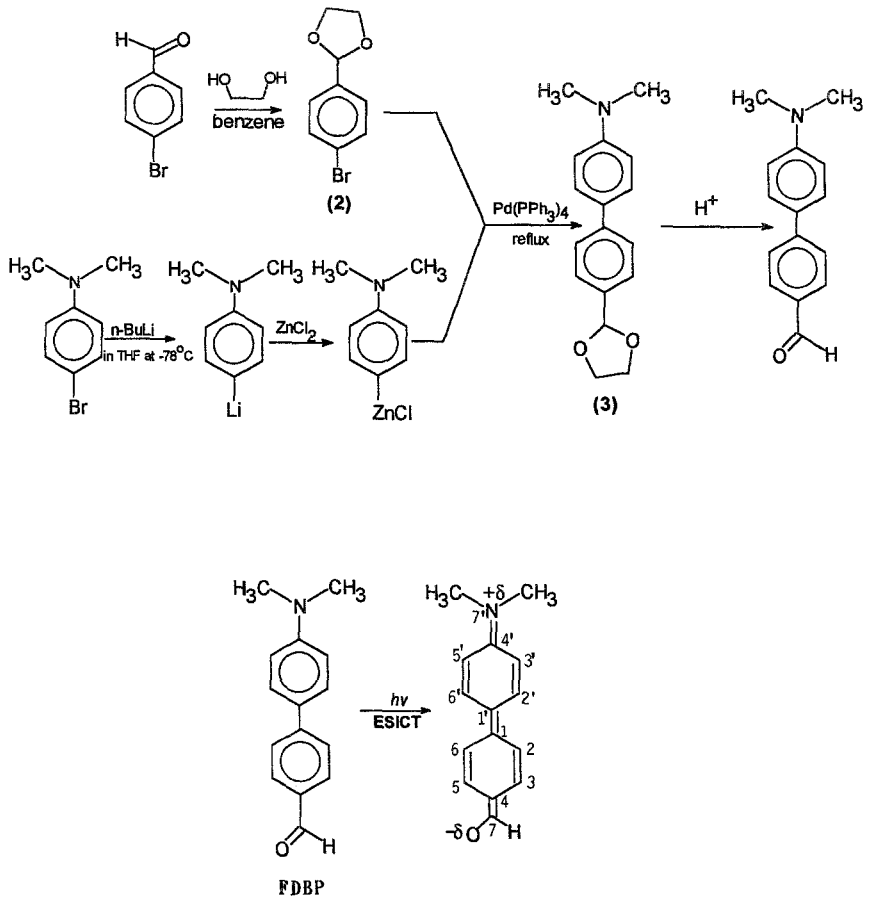

Fig. 2. The synthesis scheme of FDBP and its ESICT species. Note that the structure of the ESICT species is simply a resonance description of the degree of double-bond character, which varies with solvent polarity.

different electronic states, the neutral and charge transfer states. As a result, molecular electronic devices (bistable switches) based on the charge transfer system may be feasible. In this paper, we report the synthesis and spectroscopic studies of 4-formyl-4'-*N*,*N*-dimethylamino-1,1'-biphenyl (FDBP; Fig. 2). Our goal is to study the ESICT properties of this single donor/acceptor-substituted biphenyl system and use it as a model to test the suitability of the ultimate polyaromatic structure **1**. This seminal study presents the exploration of several unusual photophysical properties of FDBP due to strong charge transfer properties in the excited state as opposed to weak donor/acceptor coupling in the ground state.

EXPERIMENTAL

Measurement. Steady-state absorption and emission spectra were recorded with an HP (Model 8452A) spectrophotometer and an Hitachi SF 4500 fluorimeter, respectively. The excitation light source was corrected with a rhodamine B quantum counter. The wavelength-dependent detectivity of the photomultiplier was calibrated by recording the scattered light spectrum of the corrected excitation light from a diffused cell in the range of 220–650 nm. The spectrum is then saved in the computer and used for future correction of the emission spectrum. Fluorescence quantum yields were measured using quinine sulfate/1.0 *N* H_2SO_4 as a reference, assuming a yield of 0.564 with 360-nm excitation [9]. Lifetime studies were performed with an Edinburgh FL 900 photon counting system with a hydrogen-filled flash lamp/or a nitrogen lamp as the excitation source. The temporal resolution after deconvolution of the exciting pulse was ~200 ps. Data were analyzed using the nonlinear least-squares procedure in combination with the deconvolution method [10].

Materials. All solvents were of spectrograde quality and purified as described previously [11]. To exclude the known presence of water, acetonitrile (Merck Inc.) was

Table I. Photophysical Properties of FDBP in Various Solvents

	E_T (30) (kcal/mol)	λ_{max} (nm) (cm^{-1}) $S_0 \rightarrow S_1$	Fluorescence	Yield (ϕ_f)	k_{obs}[a] $\times 10^{-8}$ s^{-1} (χ^2)[b]	k_r $\times 10^{-8}$ s^{-1}	k_{nr} $\times 10^{-8}$ s^{-1}
N-Heptane	31.1	365 (27,395)	390 (26,540)	0.05	—[c]	—	—
Ether	34.5	368 (27,170)	440 (22,727)	0.45	6.25 (1.10)	2.81	3.44
Ethyl acetate	38.1	372 (26,880)	475 (21,050)	0.75	3.50 (1.02)	2.62	0.88
Chloroform	39.1	375 (26,667)	485 (20,620)	0.60	3.58 (1.00)	2.15	1.44
Acetone	42.2	378 (26,455)	510 (19,610)	0.45	4.67 (1.05)	2.10	2.57
Acetonitrile	45.6	378 (26,455)	530 (18,870)	0.14	13.77 (1.07)	1.93	11.84
Ethanol	51.9	380 (26,315)	490[d] (20,410)	0.004	—[c]	—	—
Methanol	55.4	380 (26,315)	490[d] (20,410)	0.001	—[c]	—	—

[a]The excitation wavelength is monitored at the absorption maximum.
[b]The standard deviation is calculated based on a single-exponential fit.
[c]k_{obs} is larger than our detection limit of 5.0×10^9 s^{-1}.
[d]The fluorescence maximum is excitation wavelength dependent. For this case, the excitation wavelength is chosen to be 380 nm.

first dried over 4-Å Linder molecular sieves, then stored over calcium hydride. Acetonitrile was then refluxed over P_2O_5 in a dry atmosphere and distilled into the sample cell without contact with air. In all cases no fluorescence impurities were observed from the solvent blank. The solutions were either saturated with air or degassed by three freeze–pump–thaw cycles under vigorous stirring conditions on the vacuum line ($\sim 10^{-5}$ Torr). However, the observed fluorescence decay is nearly independent of oxygen concentration.

Synthesis of FDBP. A synthesis scheme for FDBP is depicted in Fig. 2, in which 4-bromobenzaldehyde was allowed to react with ethylene glycol, yielding 4-bromobenzaldehyde 1-ethylene ketal, **2**. In another reaction, 4-bromo-*N*,*N*-dimethylaniline (1 g) was reacted with *n*-butyllithium (2.7 ml of a 2 *M* solution in cyclohexane) at −78°C in THF (10 ml) for 1 h, thus forming an organolithium product. Subsequently, $ZnCl_2$ (15 ml of a 0.5 *M* THF solution) was added at −78°C and the dry ice bath was removed. The reaction mixture was allowed to warm gradually to room temperature during the course of the reaction. After a period of 1 h, 0.93 g of **2** and 0.40 g of tetrakis (triphenylphosphine) palladium (0.07 equiv) were added. The reaction mixture was refluxed for 5 h until a significant appearance of the ketal compound **3** (see Fig. 2) was observed by TLC (3:1 hexane:ethyl acetate). The mixture was filtered and dried. Exposing compound **3** to a slightly acidic aqueous environment produces the product FDBP. Column chromatography using a 3:1 hexane:ethyl acetate eluent was effective in separating the starting material from the product. Other reaction by-products were further separated using an 8:1 hexane:ethyl acetate eluent. The collected product (FDBP, 0.8 g) was then twice recrystallized using an ethanol/water (1:1, v/v) mixture. *Analyses.* ^{1}H NMR (300 MHz, $CDCl_3$): δ = 3.1 (6H), 6.65–6.70 (4H), 7.70–7.75 (4H), 10.0 (1H). IR (powder): 1702 cm^{-1} (C=O stretch); M^+z 225 (GC/MS).

RESULTS AND DISCUSSION

Solvent Effect. Table I lists the absorption and emission maxima for FDBP as a function of solvent polarity [E_T(30)]. Typical solvent-dependent absorption and emission spectra of FDBP in *n*-heptane and acetonitrile are shown in Fig. 3. Except in protic solvents (vide infra), the frequency of the emission maximum shows a linear bathochromic shift as the solvent polarity [E_T(30) scale] increases. The change in $\Delta\tilde{\nu}$ [$\tilde{\nu}_{max}$(absorption) − $\tilde{\nu}_{max}$(emission)] varies from 1500 cm^{-1} in *n*-heptane to as much as 7500 cm^{-1} in acetonitrile (see Table 1). In contrast, the absorption maximum of FDBP shows very little solvent polarity dependence. A bathochromic shift

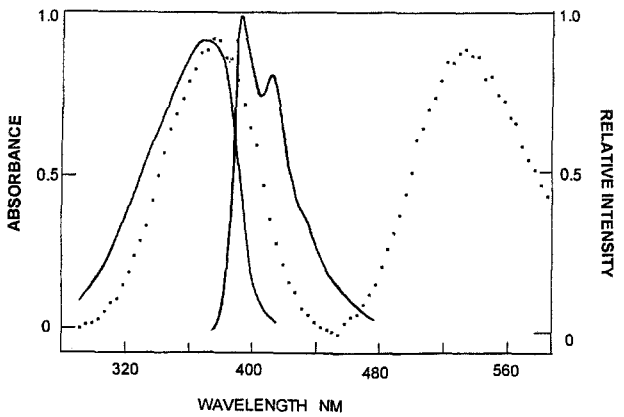

Fig. 3. Absorption and emission spectra of FDBP in (—) *n*-heptane (1.0×10^{-5} *M*) and (·····) acetonitrile (1.2×10^{-5} *M*). Excitation wavelengths of λ_{ex} = 360 and 380 nm were used in acquiring the emission spectra in *n*-heptane and acetonitrile, respectively.

of only <1000 cm^{-1} was observed from *n*-heptane (365 nm) to CH_3CN (380 nm). As a comparison, the ketal compound **3**, which is generally considered a non- or weak-charge transfer molecule, exhibits very small solvent-dependent, normal Stokes-shifted emission maxima, ranging from ~360 nm in *n*-heptane to ~380 nm in methanol (Table II). Therefore, the results of FDBP can be rationalized based on the charge transfer character in the S_1 state, induced by the electron donor (dimethylamino substituent) coupled with the electron acceptor (carbonyl oxygen). Following solvent dielectric relaxation, a large Stokes-shifted emission was observed.

The fluorescence yield, Φ_f, of FDBP is also drastically solvent polarity dependent (Table I). In nonpolar to weak polar solvents [$E_T(30)$ scale, <38 kcal/mol], Φ_f increases as the solvent polarity increases. After reaching a maximum value of 0.75 in ethyl acetate, Φ_f decreases as the solvent polarity increases. Table I also shows the measured fluorescence decay rate, K_{obs}, of FDBP in a variety of solvents. The decays are all fit well (indicated by the χ^2 value) by a single-exponential component. We also attempted to fit the decay curve by the sum of two or three decay components. However, the results are not as good as using a single-exponential fit. The observed lifetime, τ_f ($=1/k_{obs}$), against the $E_T(30)$ scale is in accord with the trend of measured Φ_f. τ_f is beyond our instrument response (200 ps) in *n*-heptane, increasing to 2.89 ns in ethyl acetate and decreasing significantly, from 0.7 ns in acetonitrile to a value of <200 ps in protic solvents. In comparison, the fluorescence yield of the non- or weak-ESICT compound **3** is high and shows a slight solvent polarity dependence (see Table II).

Apparently, for FDBP the fluorescence yields and fluorescence lifetimes are not proportional as the solvent polarity is changed. This suggests that there is either an alternation in the radiative decay, k_r, or a contribution from static (both intramolecular and intermolecular) quenching. Therefore, the values of k_r ($=k_{obs} \times \phi_f$) and k_{nr} ($=k_{obs} - k_r$) for FDBP in each solvent were calculated and are shown in Table I. Obviously, the difference in the k_r value with respect to the solvent polarity is small. For example, excluding solvents in which k_r is not obtainable due to the response-limited decay rate, the largest k_r value of 2.81×10^8 s^{-1} in ethyl ether is only 45% higher than the smallest value of 1.93×10^8 s^{-1} in acetonitrile. Therefore, the solvent-dependent fluorescence yield is attributed mainly to the nonradiative decay rate, k_{nr}, associated with the static quenching. This can be supported by the calculated k_{nr} value of 11.84×10^8 s^{-1} in acetonitrile, which is ~13 times as large as that in ethyl acetate, correlating with the ~6 times higher fluorescence yield in ethyl acetate with respect to that in acetonitrile.

The above results can be rationalized by the quenching dynamics of the excited-state charge transfer species coupled with the solvent–solute dipole–dipole interaction. Since the solvent stabilization with the charge transfer species is negligible in *n*-heptane, we expect much weaker charge transfer properties for FDBP in the excited state relative to that in polar solvents. Consequently, the C(1)–C(1'), C(4)–C(7), and C(4')–N(7') bonds of FDBP (see Fig. 2) may exhibit a more single bond-like character in nonpolar solvents than in polar media. Thus, the low-frequency torsional motion of these three bonds may serve as major deactivation channels. From another approach, the ~10 times stronger fluorescence yield in the non-or weak-ESICT compound **3** in comparison to FDBP in *n*-heptane further suggests that the major nonradiative decay channel may not be attributed to the C(1)–C(1') and C(4')–N(7') but the C(4)–C(7) torsional motion. This proposed mechanism can be rationalized by the delocalization of the carbonyl π electrons coupled with the biphenyl chromophore. Evidence of such a coupling is provided by a significant red shift (~65 nm) of the S_0–S_1 absorption maximum in FDBP (365 nm) relative to compound **3** (300 nm). Therefore, the C(4)–C(7) torsional motion directly decouples the π electron delocalization, hence inducing nonradiative deactivation. When the solvent polarity increases, stabilization of the excited-state charge transfer species leads to more C(4)–C(7) double-bond character. As a result, the radiationless decay is reduced due to the higher-frequency C(4)–C(7) torsional vibration, which is not energetically favorable to couple with the solvent

Table II. Photophysical Properties of Ketal Compound **3** inVarious Solvents

	E_T (30) (kcal/mol)	λ_{max}, nm (cm^{-1})		Yield (ϕ_f)	k_{obs} $\times 10^{-8}$ s^{-1}	k_r $\times 10^{-8}$ s^{-1}	k_{nr} $\times 10^{-8}$ s^{-1}
		$S_0 \rightarrow S_1$	Fluorescence				
n-Heptane	31.1	300 (33,333)	358 (27,933)	0.40	2.77	1.08	1.69
Ether	34.5	304 (32,895)	360 (27,777)	0.43	5.26	2.26	3.00
Ethyl acetate	38.1	304 (32,895)	365 (27,397)	0.59	6.67	3.90	2.77
Chloroform	39.1	—[a]	—[a]	—[a]	—[a]	—[a]	—[a]
Acetone	42.2	305 (32,787)	380 (26,315)	0.41	6.67	2.73	3.94
Acetonitrile	45.6	300 (33,333)	383 (26,109)	0.57	6.62	3.70	2.92
Ethanol	51.9	304 (32,895)	383 (26,109)	0.35	9.90	3.46	6.44
Methanol	55.4	304 (32,895)	383 (26,109)	0.33	10.0	3.30	6.70

[a]Due to a major photoreaction with the solvent, the photophysical data are not reported here.

deactivation channels. Instead, the solvent–solute dipole/dipole interaction plays a major role in the nonradiative relaxation dynamics in the excited state. The dynamics of quenching, resulting from the combination of these two interactions, become minimal when the solvent polarity reaches that of ethyl acetate [$E_T(30)$ = 38.5]. The observation of a >500-fold decrease in Φ_f ($\sim 1.0 \times 10^{-3}$) in methanol relative to that in ethyl acetate suggests that the solvent (–OH)–solute (–C=O and $-NR_2$) hydrogen-bonding interaction may dominate the decay dynamics of FDBP in the excited state. However, since acetone [$E_T(30)$ = 42] is a hydrogen-bond acceptor but acetonitrile [$E_T(30)$ = 46] is not, yet the k_{nr} is more rapid in acetonitrile, the hydrogen-bonding effect may not be a crucial factor. Instead, the low fluorescence yield with dominant nonradiative decay in ethanol and methanol most likely results from a specific protic solvent effect such as the nonadiabatic excited-state proton transfer from EtOH (or MeOH) to the carbonyl oxygen, which possesses more electron negativity (i.e., more basicity) in the excited state due to the charge transfer reaction.

The low fluorescence yield in protic solvents gives an explanation for the exceptional hypsochromic shift of the emission peak as opposed to the bathochromic shift in aprotic, polar solvents (see Table I). For the past several years, pico- to femtosecond time-resolved fluorescence studies of many organic dyes have clearly demonstrated emission wavelength-dependent decay dynamics in polar media due to solvent dielectric relaxation [4–6]. However, limited by the fixed excitation wavelength, these studies usually did not address the possibility of the distribution of various energies of a chromophore resulting from different environments of solute–solvent interactions, which are thermally equilibrated in the ground state. If this is the case, excitation wavelength-dependent decay dynamics should also be observed. In steady-state (non-time-resolved) measurements, the excitation wavelength-dependent fluorescence profile (the so-called red edge effect [12–16]) has been observed in solid and highly viscous glassy solutions in which the mean solvation relaxation time, τ_{sol}, is longer than the fluorescence decay time, τ_f. Since τ_{sol} ranges from 0.1 to 6.0 ps [5] at room temperature for solvents used in this study, $\tau_{sol} \ll \tau_f$ for most fluorescence dyes in these solvents. As a result, the red edge effect cannot be resolved by a steady-state measurement in such low-viscous solvents due to the dominant emission from the completely solvent-relaxed species. If the nonradiative lifetime (τ_f) of the relaxed charge transfer species is of the same magnitude as the τ_{sol} (i.e., $\tau_f \sim$ picoseconds), and the molecule has a large dipole moment change in the excited state with respect to its ground state, a steady-state excitation wavelength-dependent emission profile, i.e., a red edge effect, is expected even in solvents of a low viscosity at room temperature. Since the radiative lifetime, τ_r, of the allowed $\pi\pi^*$ transition is generally 1–100 ns for aromatic organic molecules, a τ_f of picoseconds indicates that the fluorescence yield must be very low due to the dominant nonradiative decay. Consequently, molecules that can demonstrate such a phenomenon are rare [17,18]. FDBP in methanol (or eth-

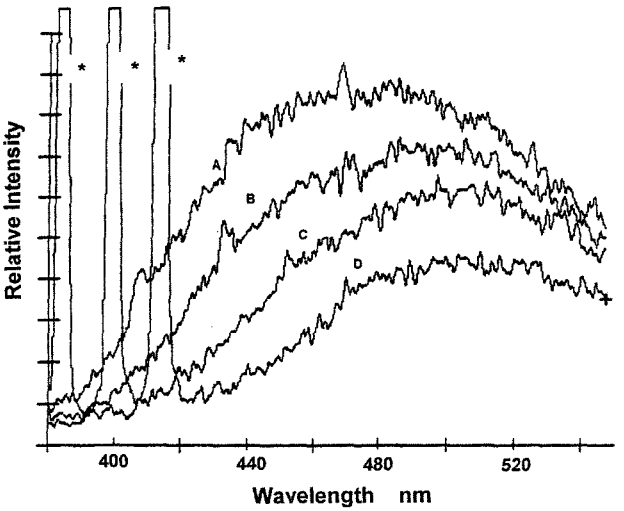

Fig. 4. Excitation-wavelength dependent emission spectra of FDBP in methanol. λ_{ex} = (A) 370 nm, (B) 385 nm, (C) 400 nm, and (D) 415 nm. Asterisks denote the Rayleigh scattering.

anol) provides a prototype example due to its strong excited-state charge transfer properties and small Φ_f of ~0.001 (τ_f is beyond the response of 200 ps of our detection system). Figure 4 clearly shows the change in the spectral features of FDBP as a function of excitation wavelength. Excitation in the shorter-wavelength region of the S_0–S_1 absorption band corresponds to a greater hypsochromic shift of the emission peak. As a result, the abnormal higher peak frequency (λ_{max} = 490 nm on 380-nm excitation; see Table 1) in methanol (or ethanol) relative to that in acetonitrile (λ_{max} = 530 nm) can be rationalized due to the higher-frequency emission during solvent dielectric relaxation. It should be noted that the observed excitation-dependent red edge effect observed in protic solvents may also possibly be due to the absorption transitions to two close lower-lying excited states (as in the ^1L_a and ^1L_b transitions of indole [19,20]). Thus, the excitation into the overlapping different energy levels results in the observed change in the emission maximum. Experimentally, this could be tested by measuring the excitation spectra at different polarizer settings to obtain independent spectra from each transition. In a steady-state approach, the experiment can be carried out with a highly viscous media, i.e., ethylene glycol at a medium-low temperature, in which the averaged time required for solvation relaxation is slower than the sample decay dynamics. Unfortunately, FDBP exhibits negligible fluorescence intensity in ethylene glycol. We are currently setting up a subpicosecond detection system to resolve this question based on time-resolved fluorescence anisotropy measurement.

Lasing Properties. On the basis of the high-yield and large Stokes-shifted fluorescence properties, amplified spontaneous emission (ASE) was observed for FDBP in several polar, aprotic solvents, including diethyl ether, ethyl acetate, chloroform, and acetone. The wavelength-dependent gain coefficients (α) were determined based on a previously reported method [21,22] using the third harmonics (355 nm, 10 ns) of the Nd:YAG laser as a pump pulse. By measuring the intensity I_L for ASE from the full cell length L and the intensity $I_{L/2}$ from the cell half-length, one can evaluate the gain coefficient α at a given wavelength using $\alpha = 2/L \ln[(I_L/I_{L/2}) - 1]$. The gain coefficient was experimentally determined to be 8.6 ± 0.8, 9.2 ± 0.7, and 9.0 ± 0.8 at ASE maxima of 445, 476, and 485 nm in ethyl ether, ethyl acetate, and chloroform, respectively. Under identical conditions, the α value was measured as 9.3 ± 0.5 at 400 nm for a commercially available laser dye, Exalite 398, indicating that the laser gain coefficient of FDBP in these three solvents is comparable with that of the regular laser dye. Since the duration (~10 ns) of the pump pulse is much longer than the fluorescence decay of FDBP in the studied solvents, the higher pumping threshold power is required for the shorter fluorescence decay species. Therefore, this comparison is only qualitative. However, even in acetone, in which the fluorescence yield of FDBP is relatively low (Φ_f = 0.2), a high-gain ASE (α = 8.3 ± 0.6) was still observed, indicating that the ground-state reabsorption is negligibly small due to the large Stokes-shifted charge transfer emission.[5] We also utilized a Quanta-Ray PDL-1 dye laser containing a side pump and end pump configuration to measure the output of laser intensity, and monitored both third-harmonic (355-nm) and dye laser output powers using a Gentec ED-200 joule meter. Figure 5 displays the dye–laser tuning curve for FDBP in ethyl acetate. Under optimized conditions, 2.6 mJ/pulse was achieved at 476 nm when pumped by 25 mJ of a 355-nm pulse. This corresponds to a conversion efficiency of ~10%, which is comparable with the efficiency that commercial laser dyes can achieve. A similar output efficiency was obtained in diethyl ether and chloroform. The tunability of 438–450, 472–483, and 480–490 nm in ethyl ether, ethyl acetate, and chloroform, respec-

[5] We also performed triplet–triplet absorption measurement. However, negligible triplet–triplet absorbance in the region of 400–500 nm was observed. Therefore, we also concluded that triplet–triplet absorption does not play an important role in quenching the lasing action.

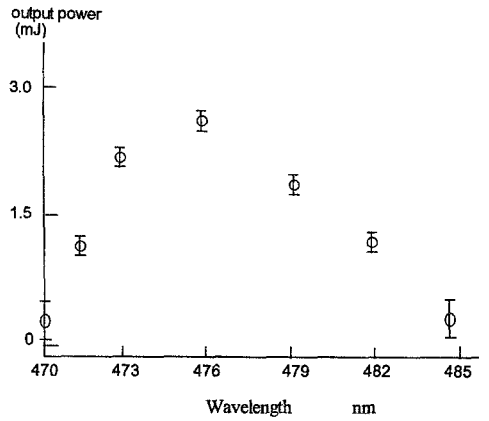

Fig. 5. Dye–laser tuning curve for FDBP in ethyl acetate, pumped by a 355-nm Nd:YAG laser (25 mJ/pulse).

tively, leads to the development of a new solvent-dependent charge transfer laser dye in the blue–green region.

CONCLUSION

In conclusion, synthesis of FDBP provides versatile applications. Due to the high fluorescence yield (in medium polar solvents) and large Stokes-shifted emission, lasing action was also observed, leading to a polarity-dependent lasing frequency covering the blue–green region (430–490 nm). Our results also unambiguously show the red edge effect in low-viscous protic solvents. Consequently, FDBP serves as an ideal fluorescence probe to study solvation dynamics, and significant time-dependent (possibly followed the solvent dielectric relaxation) Stokes shifts should be observed for the charge transfer emission in various polar solvents. The strong excited-state charge transfer property may lead to the ultimate design of feasible donor/acceptor-coupled polybiphenyl structure **1**. Research focusing on this is currently in progress.

ACKNOWLEDGMENTS

Start-up support from the National Chung-Cheng University is graciously acknowledged. This work was partially supported by the National Science Council, Taiwan, R.O.C.

REFERENCES

1. K. Rotkiewicz, K. H. Grellmann, and Z. R. Grabowski (1973) *Chem. Phys. Lett.* **19**, 315–318.
2. Z. R. Grabowski, K. Rotkiewicz, A. Siemiarczuk, D. J. Cowley, and W. Baumann (1979) *Nouv. J. Chim.* **3**, 443–454.
3. E. Lippert, W. Rettig, V. Bonacic-Koutecky, F. Heisel, and J. A. Miehe (1987) *Adv. Chem. Phys.* **68**, 1–173.
4. J. D. Simon (1988) *Accounts Chem. Res.* **21**, 128–134; and references therein.
5. P. F. Barbara and W. Jazeba (1990) *Adv. Photochem.* **15**, 1–68, and references therein.
6. M. Maroncelli, J. MacInnis, and G. R. Fleming (1989) *Science* **243**, 1674–1681.
7. W. Rettig (1988) *Appl. Phys. B* **B45**, 145–149.
8. L. Z. Stolarczyk and L. Piela (1984) *Chem. Phys.* **85**, 451–460.
9. J. N. Demas and G. A. Crosby (1971) *J. Phys. Chem.* **75**, 991–1024.
10. D. V. O'Connor and D. Phillips (1984) *Time-Correlated Single Photon Counting*, Academic Press, New York.
11. W. E. Brewer, S. L. Studer, M. Standiford, and P. T. Chou (1989) *J. Phys. Chem.* **93**, 6088–6094.
12. W. G. Galley and R. M. Purkey (1970) *Proc. Natl. Acad. Sci. USA* **67**, 1116–1121.
13. K. A. Al-Hassan and M. A. El-Bayoumi (1980) *Chem. Phys. Lett.* **76**, 121–124.
14. R. B. Macgroger and G. Weber (1981) *Ann. N.Y. Acad. Sci.* **366**, 140–154.
15. A. P. Demchenko (1986) *Ultraviolet Spectroscopy of Proteins*, Springer-Verlag, Berlin, Chap. 7.
16. A. P. Demchenko and A. I. Sytnik (1991) *Proc. Natl. Acad. Sci. USA* **88**, 9311–9314.
17. J. Paczkowski and D. C. Neckers (1991) *J. Photochem. Photobiol.* **A62**, 173.
18. W. Retig (1980) *J. Luminesc.* **26**, 21.
19. R. L. Rich, Y. Chen, D. Neven, M. Negrerie, F. Gai, and J. W. Petrich (1993) *J. Phys. Chem.* **97**, 1781.
20. F. Gai, R. L. Rich, and J. W. Petrich (1994) *J. Am. Chem. Soc.* **116**, 735.
21. P. T. Chou, D. McMorrow, T. J. Aartsma, and M. Kasha (1984) *J. Phys. Chem.* **88**, 4596–4599.
22. C. V. Shank (1975) *Rev. Mod. Phys.* **47**, 649–657.